



# Spatiotemporal monitoring and change detection of vegetation cover for drought management in the Middle East

Elaheh Ghasemi Karakani<sup>1</sup> · Arash Malekian<sup>1</sup> · Soroush Gholami<sup>2</sup> · Junguo Liu<sup>3</sup>

Received: 3 April 2020 / Accepted: 25 January 2021 / Published online: 4 February 2021  
© The Author(s), under exclusive licence to Springer-Verlag GmbH, AT part of Springer Nature 2021

## Abstract

The Middle East (ME), as an arid and semi-arid region, is prone to environmental risks and stresses, such as drought are inseparable phenomena of the region. In this study, an approach for identifying sustained vegetation cover (SVC) is suggested to identify the connection between SVC and drought. Normalized difference vegetation index (NDVI) and land surface temperature (LST) were used to filter zones of rich vegetation cover from poorly vegetated or non-vegetated regions of the ME. The change detection of vegetation cover was computed by the NDVI differencing technique, and the vegetation condition index (VCI) and normalized vegetation supply water index (NVSWI) were used to derive drought indices. The standardized precipitation index (SPI) and rainfall anomaly index (RAI) were used to monitor the intensity of meteorological drought events. A comparison of the estimates of vegetation change, remote sensing-based VCI, and meteorological drought indices revealed that the highest SVC is concurrent with the occurrence of drought. Moreover, it was found that the most severe meteorological drought and VCI-based drought condition occurred in 2008 and that the highest percentage of SVC was also obtained for this year. The results suggest the possibility of using the SVC instead of other spectral indices, such as the NDVI, VCI, NVSWI, and NVSWI, for the superior assessment and detection of environmental stresses such as drought.

**Keywords** Environmental change detection, · Drought assessment, · Vegetation cover, · Middle East

## 1 Introduction

Drought and other environmental stresses are common threats in the Middle East (ME). Drought occurs frequently in many countries of this region and affects the lives of millions of people (Shetty 2006; World Bank, 2014). It is also an important

controlling mechanism for the management of water resources (Kaniewski et al. 2012; Van Lanen et al. 2013; Zarei et al. 2020). Several studies have indicated increasing temperatures and shifts in precipitation patterns that lead to extreme weather events, such as severe droughts, heat waves, sandstorms, and vegetation cover degradation (Kafle and Bruins 2009; Al-Qinna et al. 2011). The reduced rainfall and severe heat extremes in the ME, as in many other regions of the world, have made the region a hot spot for [climate change](#) issues (Giorgi and Lionello 2008). A drying trend has been forecasted from model projections for much of this region due to predictions of large elevations in temperature and reductions in precipitation in the near future (Bucchignani et al. 2018). The climate of most counties in this region is arid and semi-arid, and the vegetation cover is highly sensitive to drought (Abbas et al. 2014; Barlow et al. 2016). Barlow et al. (2016) explained that the vegetation cover condition in the ME is strongly controlled by the distribution of precipitation and that droughts have an obvious influence on the vegetation cover and its variability over the region. Additionally, Zaitchik et al. (2007) revealed a quick and considerable response of vegetation cover to climate variability, such as droughts and heat waves. Several remote sensing-based indices, such as the vegetation condition

---

✉ Arash Malekian  
malekian@ut.ac.ir

Elaheh Ghasemi Karakani  
ghasemi.elaheh.k@ut.ac.ir

Soroush Gholami  
s.gholamy@modares.ac.ir

Junguo Liu  
liujg@sustech.edu.cn

<sup>1</sup> University of Tehran, Tehran, Iran

<sup>2</sup> Tarbiat Modarres University, Tehran, Iran

<sup>3</sup> School of Environmental Science and Engineering, Southern University of Science and Technology, Shenzhen 518055, China

index (VCI), temperature condition index (TCI) (Kogan 1995), and vegetation supply water index (VSWI) (Carlson et al. 1994), have already been developed to represent drought effects under different climatic and environmental conditions (Wan et al. 2004; Abbas et al. 2014; Dutta et al. 2015; Sruthi and Aslam 2015; Trisasonko et al. 2015; Khosravi et al. 2017). The normalized difference vegetation index (NDVI) is the most widely operational vegetation index among the large number of indices (Bannari et al. 1995; Sruthi and Aslam 2015). This method has been used to extract differences in vegetation cover (Richards and Jia 2006), which can be defined simply to analyze seasonal, annual, and long-term vegetation cover, as well as structure, variation, etc. (Xie et al. 2008). The fraction of absorbed photosynthetically active radiation (FAPAR) anomaly is a drought-related MODIS image indicator that has been used to identify and recognize the influences of agricultural drought on the growth and productivity of vegetation in Europe (Sepulcre-Canto et al. 2012). The NDVI differencing is another vegetation index obtained by subtracting the NDVI of two consecutive dates of images that can represent the vegetation change and its relationship with drought indices (Cakir et al. 2006). Moreover, the strong correlation between NDVI and land surface temperature (LST) enables much more accurate detection of drought events (Karnieli et al. 2010; Sruthi and Aslam 2015). In most studies, the NDVI is considered to be in the range of  $-1$  to  $+1$  (Myneni et al. 1995). However, satellite-derived drought index values in most parts of arid regions have corresponded to very low values of NDVI, such as those of various geomorphic features (e.g., deserts and water bodies) or areas without notable vegetation cover. In other words, such features are categorized by negative or low values of VLC and VSWI, which are not significant for representing drought indices, and show NDVI values lower than 0.2, whereas the general range for green vegetation cover is between 0.2 and 1 (Al-doski et al. 2013; Gandhi et al. 2015; Qader et al. 2016). Therefore, this study attempted to focus on areas where NDVI values are greater than 0.2, and each pixel greater than the 0.2 threshold is to be consecutive over the available long-term MODIS satellite data. Such pixels meeting these two criteria are referred to as sustained vegetation cover (SVC) in this study and used to identify the relationship between the time series of SVC and the spectral parameters of vegetation cover and rainfall deficiency-based drought indices for possible replacement of other indices by SVC.

## 2 Materials and methods

### 2.1 Study area

The Middle East (ME) is a diverse geographical region with a total area of approximately 7.2 million km<sup>2</sup> located in southwestern Asia and northeastern Africa. The topography of the region is complex, including several deserts and high

mountains in Iran and Turkey, and most of the land is classified as arid or semi-arid (Gophen 2008; Barlow et al. 2016). This region extends from northeast Africa, through Egypt, the east coast of the Mediterranean Sea through Iran, and throughout the Arabian Peninsula (Fig. 1). It has an estimated population of about 450 million (UN 2015). Temperature and precipitation vary considerably throughout the region and even within countries. The Black Sea in Turkey and the Caspian Sea coasts in northern Iran receive about 2000 mm of annual precipitation, whereas the central desert regions of the ME often receive no or very low rainfall. This indicates that the distribution of precipitation is closely dependent on topography, especially in mountainous areas where precipitation occurs mostly during the cold season due mainly to the orographic effects of eastward storms (Barlow et al. 2016). Climate conditions in the ME vary greatly based on the geography and season. Some areas have a Mediterranean-type climate, and the well-watered highlands of Turkey and the Iran mountains are important as resources for the major rivers of this region. The hot and arid, or desert, climate predominates in many other parts of the region, especially in many Arabian countries where the climate is fairly consistent throughout the year and there are only two distinct seasons (Hasanean 2004).

### 2.2 Data and pre-processing

In this study, we used Moderate Resolution Imaging Spectroradiometer (MODIS) sensor products as satellite data to derive the NDVI and LST, including the ERA-Interim precipitation data. We obtained the MOD13C2 version 6 NDVI (details in Didan et al. 2015) for NDVI and also the MOD11C3 LST products (Wan 2008), which provide a long time series (Feb 2000–Dec 2017) of monthly LST and NDVI of the entire globe in a CGM granule (consists of a geographic grid with 7200 columns and 3600 rows representing the entire globe). Moreover, the 5600 m spatial resolution is adequate for the entire study area. The daily precipitation over the study period was derived from the ERA-Interim reanalysis dataset of the European Centre for Medium-Range Weather Forecasts (ECMWF) (Dee et al. 2011) with a spatial resolution of 0.75°. The NDVI, LST, and precipitation data of the ECMWF used in this study are freely available from the following sources: <https://earthexplorer.usgs.gov/> and <https://apps.ecmwf.int/datasets/data/interim-full-daily/levtype=sfc/>.

NDVI values range between  $+1.0$  and  $-1.0$ , where values close to  $+1$  represent stronger near-infrared reflectance that is close to photosynthesizing vegetation (Myneni et al. 1995). NDVI values less than 0.2 correspond to sand, barren areas, rock, and non-vegetated land, and negative NDVI values indicate rivers, wetlands, and snow. NDVI values greater than 0.2 indicate sparse, moderate, and dense vegetation cover (Al-doski et al. 2013; Gandhi et al. 2015; Qader et al. 2016). To focus on vegetation cover, the pixel scale from 0.2–1 was used

for extracting SVC, drought indices, and vegetation change detection, and the NDVI differencing technique was applied as a radiometric approach to vegetation change detection and land cover types (Lu et al. 2004; Pu et al. 2008b; Mancino et al. 2009; Al-doski et al. 2013). In this technique, cell-by-cell NDVI remotely sensed imagery is compared to detect

differencing images for mapping change/no-change pixels in a time series (Eq. 1) (Cakir et al. 2006; Pu et al. 2008a).

$$\Delta\text{NDVI} = \text{NDV}_{\text{year } n_i} - \text{NDV}_{\text{year } m_i} \quad (1)$$

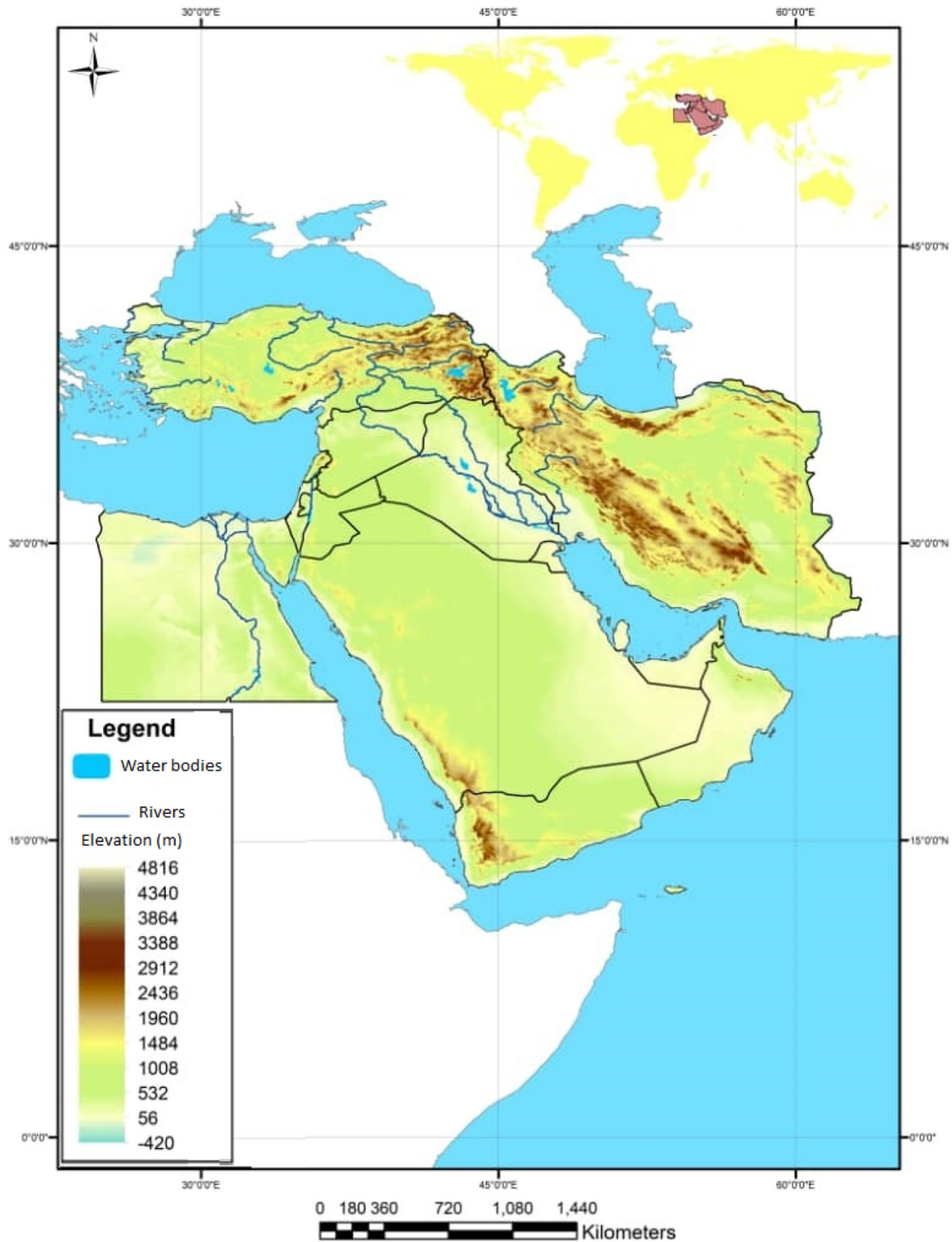


Fig. 1 Delineation of the Middle East as the study region

**Table 1** Classification of vegetation condition index (VCI) (Kogan 1995)

VCI range	Classification
50-100%	Normal condition of vegetation
35-50%	Drought condition
< 35%	Severe drought condition

The vegetation change in an image of a different date is represented by a threshold that is based on the standard deviation (SD) and mean of the NDVI differencing image, which is a commonly used technique for determining vegetation change (Singh 1989; Coppin et al. 2004; Lu et al. 2004). The images of two specific data of a time series are subtracted, and then the first standard deviation  $\mu \pm 1 \sigma$  is selected for the positive (NDVI increase) and negative (NDVI decrease) thresholds to identify changes in each pixel, while the pixels within the two derived tails characterize the condition of no change (Mancino et al. 2014). In this study, the NDVI differencing method was used to present change/no-change maps for each year by applying the standard deviation (SD) method (Rahimi et al. 2018).

Vegetation indices are useful tools for indicating drought-related vegetation conditions (Huang et al. 2014). We used the vegetation condition index (VCI) and normalized vegetation supply water index (NVSWI) as vegetation indicators in this study. The VCI has been applied widely in different climatic conditions to calculate agricultural and meteorological droughts based on the min–max normalization approach (Eq. 2.) (Kogan 1995; Khosravi et al. 2015; Magno et al. 2018), where  $NDVI_{max}$  and  $NDVI_{min}$  are the absolute maximum and minimum NDVI values of each month and for each pixel,  $j$  is the index representing the current month, and the range of VCI values is between 1–100 (Dutta et al. 2015). The VCI normalizes the NDVI, detects the short-term climate signal from the long-term vegetation, and provides a better index for evaluation of water stress than the NDVI. The classification of the VCI based on the drought severity classes proposed by Kogan (1995) is shown in Table 1.

**Table 2** Classification of normalized vegetation supply water index (NVSWI) (Dutta et al. 2015)

NVSWI range	Classification
zero	Severest drought
<20%	Severe drought
20–40%	Moderate drought
40–60%	Slight drought
60–80%	Normal
>80 %	Wet

**Table 3** Classification of SPI (McKee et al. 1993)

SPI value	Category	SPI value	Category
>0.2	Extremely wet	<-0.2	Extremely Dry
1.5–1.99	Very wet	-1.5 to -1.99	Very Dry
1.0–1.49	Moderately wet	-1 to -1.49	Moderately Dry
-0.99 to 0.99		Near Normal	

$$VCI_i = \frac{NDVI_i - NDVI_{min}}{NDVI_{max} - NDVI_{min}} * 100 \quad (2)$$

The vegetation supply water index (VSWI) is a useful approach for detecting agricultural drought. Considering the water in the canopy, partial closing of leaf stoma leads to decreased evapotranspiration, increased LST, and NDVI that is reduced by the drooping of leaves, which depends on leaf health (Eq. 3.) (Cai et al. 2010; Dutta et al. 2015).

$$VSWI = NDVI / LST(T_s) \quad (3)$$

In Eq. (3),  $T_s$  is the crop canopy temperature in the field, which can be perceived as the LST calculated from remote sensing data (Abbas et al. 2014). Despite the complex or indirect relationship between drought severity and VSWI, the index provides a simple and applied measure for soil moisture and drought monitoring (Gao et al. 2008; Dutta et al. 2015). The normalized VSWI (NVSWI) values also allow comparisons over the study period (Eq. 4.).

$$NVSWI = \frac{VSWI_{max} - VSWI}{VSWI_{max} - VSWI_{min}} * 100 \quad (4)$$

Here, NVSWI is the normalized VSWI, VSWI max, and VSWI min are the respective values of each pixel over the period of study, and VSWI is the index of the current month. The range of this index is from 0 to 100, depending on drought conditions (Table 2).

We also considered meteorological indices, including the standardized precipitation index (SPI) (McKee et al. 1993) (Table 3) and the rainfall anomaly index (RAI) introduced by Van Rooy (1965) to assess the performance of the SVC. The RAI, as a simple and efficient drought index, was used to analyze the intensity and frequency of wet and dry years (Eq. 5).

$$RAI = R - \mu / \quad (5)$$

In Eq. (5), RAI is the rainfall anomaly index,  $R$  is rainfall,  $\mu$  is the long-term average rainfall, and  $r$  is the standard deviation. The rainfall anomaly of each year in this study was calculated based on the long-term average rainfall (Table 4).

**Table 4** Classification of rainfall anomaly index (Van Rooy 1965)

RAI range	Classification
Above 4	Extremely humid
2 to 4	Very humid
0 to 2	Humid
-2 to 0	Dry
-4 to -2	Very dry
Below -4	Extremely dry

The mean monthly precipitation of the ERA-Interim was used to calculate the annual SPI and RAI in the current work.

### 3 Results and discussion

Some studies have considered NDVI values between -1 and +1, but there are arid and semiarid regions in the ME that are classified mostly as barren regions and are outside of

phenological detection. Therefore, the threshold of 0.2 was applied to denote zones of plants with good condition and to provide an opportunity to trace SVC and vegetation change detection and classification of vegetation-related indices obtained by this threshold. Figure 2 shows the percentage of total area attributed to NDVI > 0.2 in each year throughout the study area. As shown, high NDVI dominance occurred in April, May, and June, in accordance with the growing season.

#### 3.1 Vegetation land cover (VLC) and long-term sustained NDVI

The 0.2 threshold of monthly NDVI was calculated over the study period, and Fig. 3 shows the interquartile range of VLC by long-term NDVI > 0.2 for the region. The box plots for the 25th and 75th percentile thresholds of the area and the median of VLC by NDVI > 0.2 distributions reveal differences in the countries and the whole region. For most countries, the whiskers of the box plots are apparently much higher in January, February, March, and April than in other months, but for

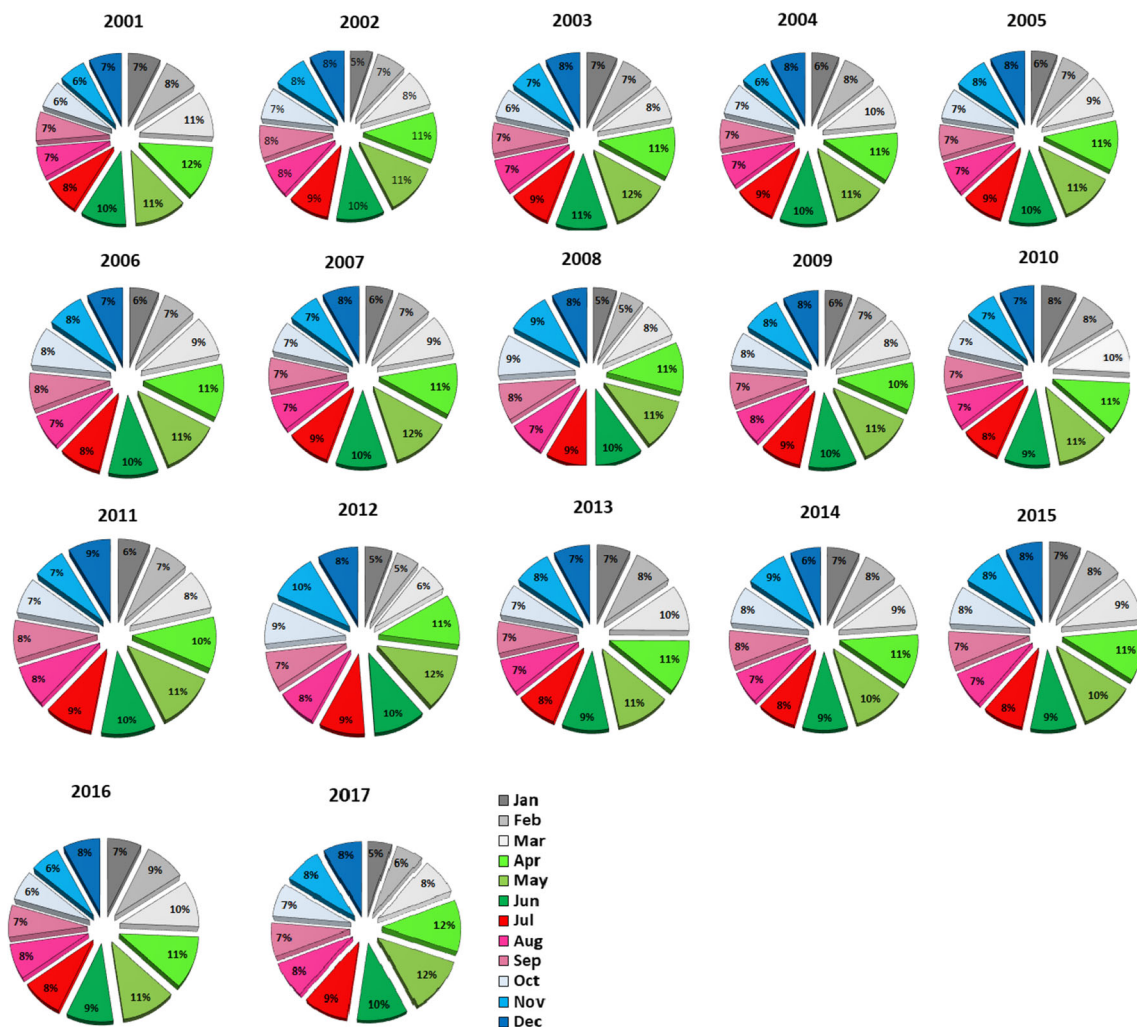


**Fig. 2** Pie chart showing distribution of area attributed to NDVI > 0.2 in each year over 2001–2017

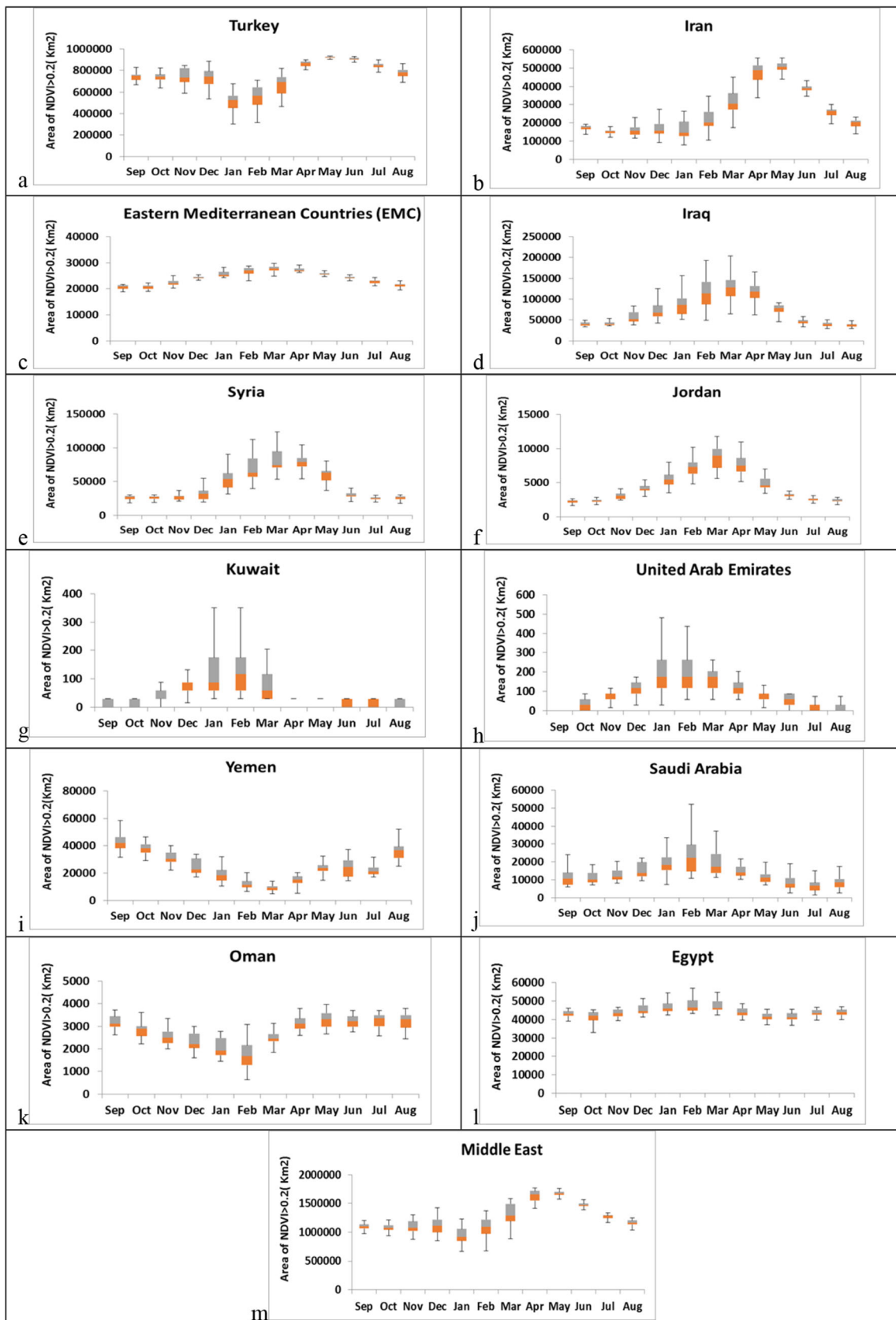


**Fig. 3** Distribution of vegetation cover (VC) with NDVI > 0.2 in the Middle East countries; the orange box shows the 25th percentile, the gray box represents the 75th percentile; the bold horizontal line represents the

median and the whiskers of the box plots extend to the maximum and minimum values of distribution in filtering zone of the study region

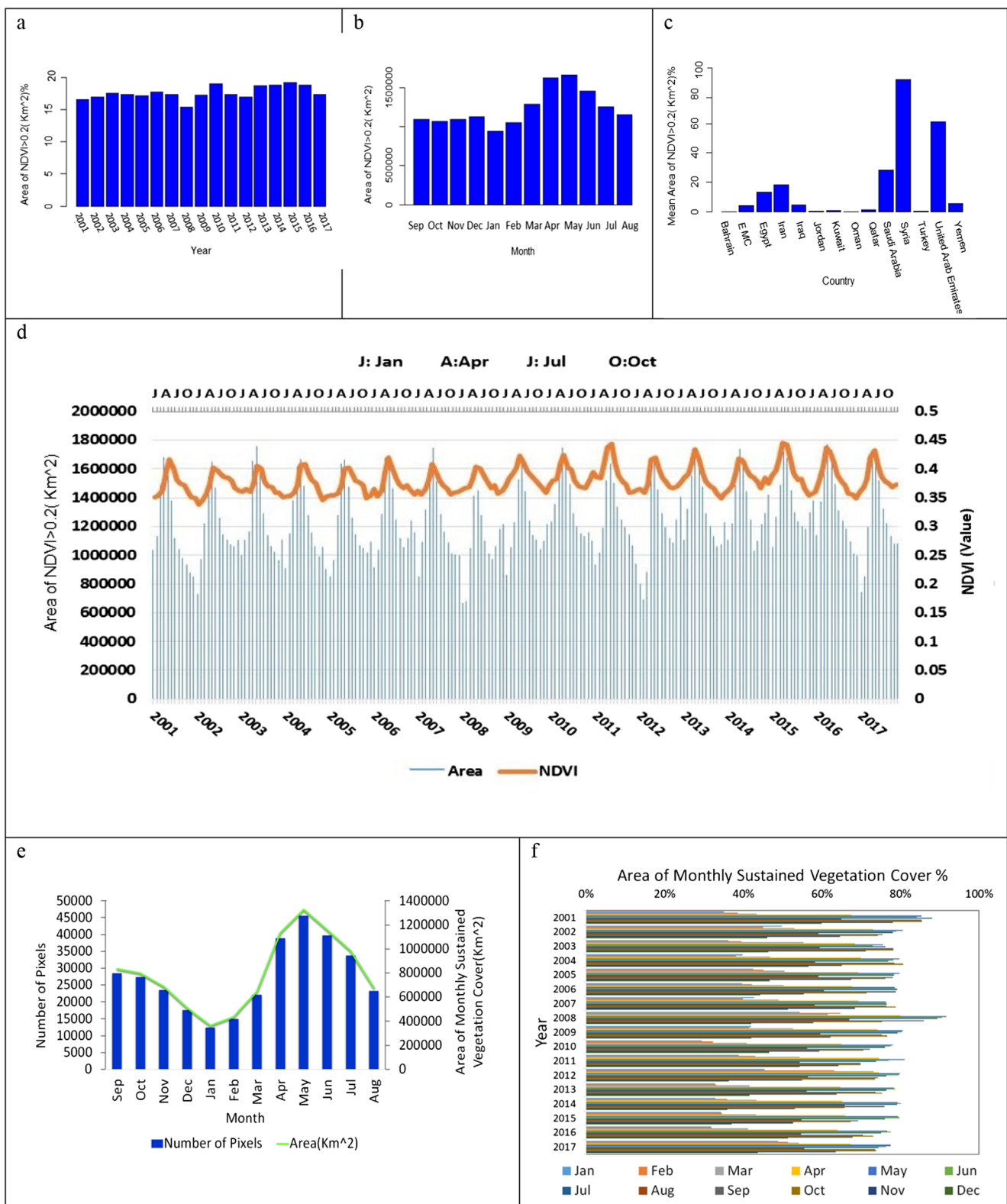


**Fig. 4** **a** Average of monthly changes in vegetation cover in the ME. **b** The percentage of time changes on vegetation land cover in the ME. **c** Ratio of vegetation land cover in each country. **d** Averaged NDVI monthly and vegetation land cover in the filtering zone of the study area. **e** Averages of pixels' number and area of monthly sustained vegetation cover. **f** The ratio of sustained vegetation area in each year in the filtering zone of the study area

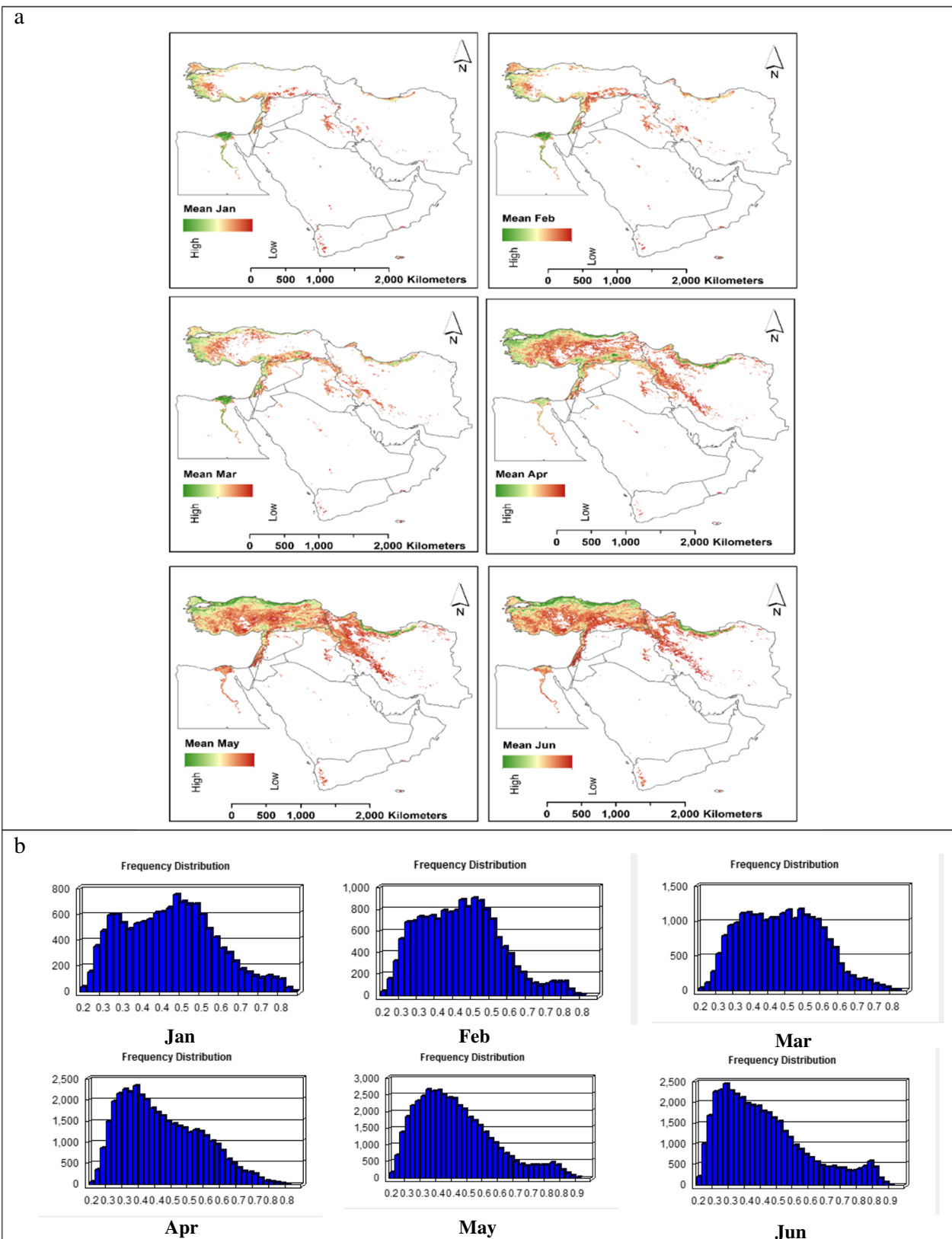


**Fig. 5 a** Thematic maps showing selected pixels of sustainable NDVI and spatial extend of monthly mean pixels' value. **b** Frequency distribution of pixels (Jan ...Jun) in the filtering zone of the study area.

**c** Thematic maps showing selected pixels of Sustainable NDVI and spatial extend of monthly mean pixels' value. **d** Frequency distribution of pixels (Jul ... Dec) in the filtering zone of the study area

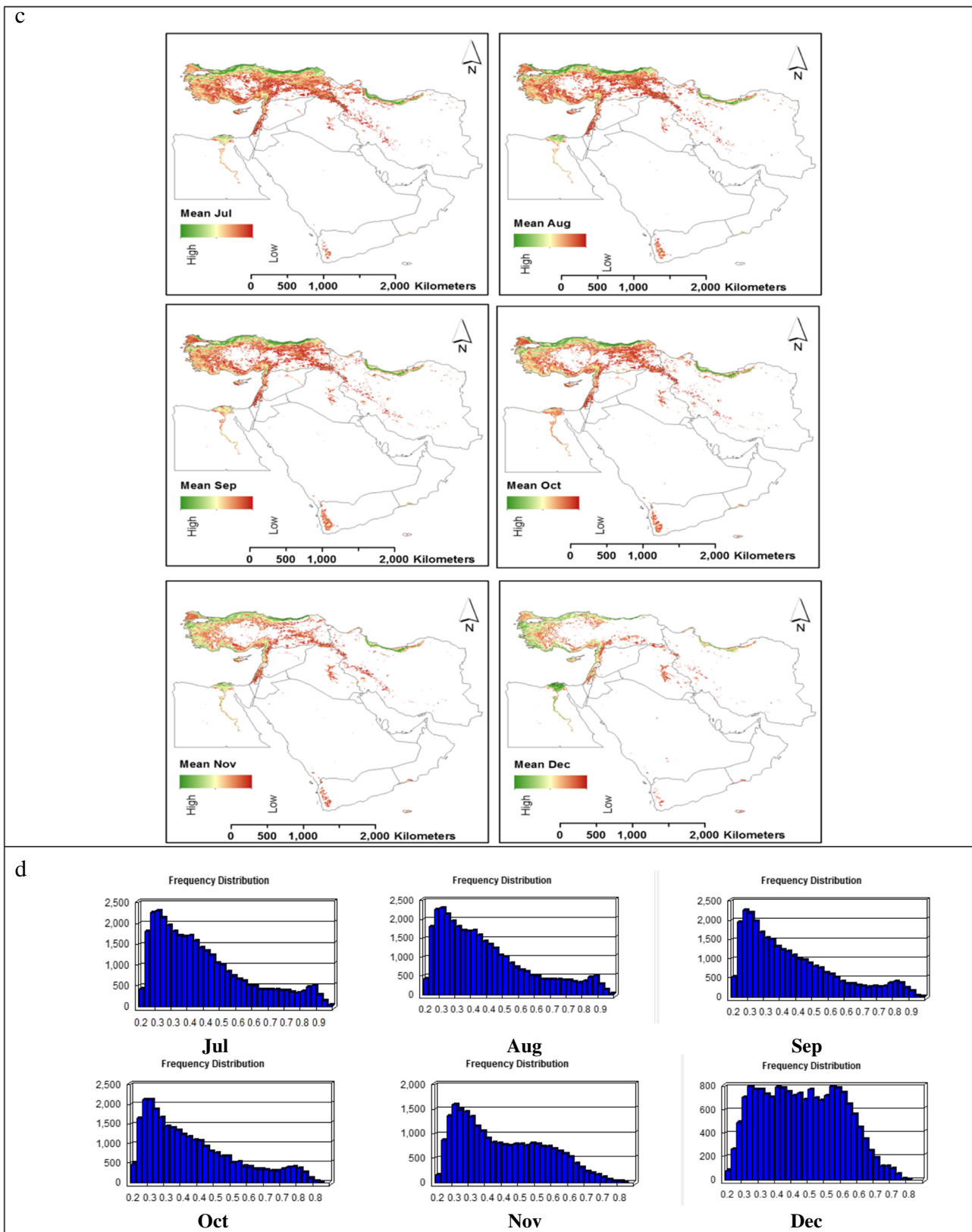
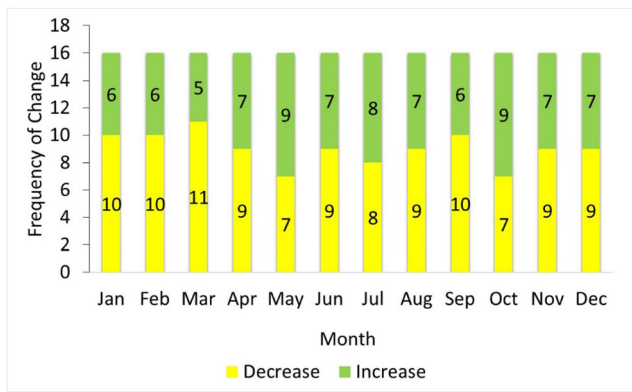


Fig. 5 (continued)

**Table 5** NDVI differencing area in percentage over the study period

Year	Jan		Feb		Mar		Apr		May		Jun		Jul		Aug		Sep		Oct		Nov		Dec		Mean		Change
	Incr.	Decr.																									
2002-2001	7.0	11.8	9.4	11.7	10.9	13.1	11.8	13.0	12.8	13.7	10.2	10.9	11.4	8.8	11.4	8.0	12.2	8.5	14.8	10.6	15.0	9.9	13.7	9.2	11.7	10.8	+
2003-2002	14.4	8.8	14.0	11.6	10.7	12.8	11.6	12.2	11.0	10.0	9.1	8.6	8.6	12.7	8.8	12.6	8.8	13.2	9.6	14.9	10.2	13.6	10.4	12.4	10.6	11.9	-
2004-2003	10.3	10.5	12.1	13.2	13.6	11.0	13.9	12.2	12.1	11.5	10.0	9.2	12.5	8.7	12.9	9.1	12.0	8.5	10.6	11.7	11.3	12.9	10.5	11.0	11.8	10.8	+
2005-2004	9.1	11.0	10.1	12.9	11.1	12.4	12.4	10.7	10.6	11.4	8.4	8.8	9.5	10.1	10.0	10.8	10.1	10.6	12.7	10.6	11.9	13.1	12.0	9.8	10.5	11.0	-
2006-2005	11.4	10.4	12.4	11.7	11.7	12.0	12.7	12.0	12.3	10.1	7.8	10.0	9.1	10.6	9.1	11.7	7.9	10.8	12.6	11.4	14.5	11.4	13.4	9.9	11.1	11.0	+
2007-2006	11.0	11.5	11.1	12.0	12.1	12.1	12.6	13.2	11.5	11.3	9.6	10.5	11.8	9.9	11.5	9.6	11.0	10.5	11.3	16.3	11.9	13.9	10.9	13.1	11.2	12.0	-
2008-2007	8.1	11.6	8.9	12.8	10.8	12.8	11.4	12.5	9.1	12.6	10.6	14.1	10.3	13.5	10.0	13.3	11.1	13.2	14.4	13.0	13.2	11.5	11.8	10.3	10.9	12.6	-
2009-2008	13.0	10.3	13.6	11.3	13.5	10.7	13.6	11.5	12.3	9.7	11.1	9.6	10.5	10.3	12.4	8.7	14.0	9.4	12.9	12.4	12.5	12.8	13.2	12.2	12.5	10.8	+
2010-2009	14.1	11.8	13.2	12.4	11.7	10.8	11.5	11.4	12.1	11.2	8.9	10.1	10.9	9.9	10.3	10.9	8.5	10.2	13.2	12.8	13.3	12.2	12.1	11.9	11.6	11.3	+
2011-2010	11.7	14.7	11.4	14.0	11.2	13.3	12.5	13.9	11.5	10.8	12.9	9.9	11.0	9.5	12.1	11.4	12.2	11.4	11.8	10.8	10.9	12.4	11.2	14.0	11.9	12.2	-
2012-2011	12.5	14.5	8.9	12.9	11.4	14.4	12.8	14.0	11.6	14.0	9.5	12.2	9.6	9.7	10.4	11.0	11.1	11.6	9.7	11.9	10.9	9.8	13.8	8.7	10.9	12.0	-
2013-2012	13.6	9.4	15.7	10.7	15.1	14.4	14.1	12.8	13.1	11.3	9.6	9.9	10.1	11.7	10.2	11.2	9.5	11.2	11.2	11.3	13.0	14.3	10.5	13.4	12.2	11.8	+
2014-2013	10.5	13.7	10.4	13.9	11.5	13.8	11.6	12.9	9.4	11.9	9.8	10.2	11.8	11.1	9.4	8.6	12.5	9.3	14.5	12.0	13.8	11.9	10.5	11.4	11.6	11.7	-
2015-2014	14.0	10.6	14.7	11.9	14.2	11.9	14.1	12.4	14.3	9.5	11.3	10.0	14.4	11.7	7.9	8.8	10.4	10.4	12.5	11.4	11.7	12.6	12.3	13.6	12.5	11.2	+
2016-2015	11.3	13.9	11.1	15.0	11.1	13.0	11.5	12.2	10.5	13.2	10.8	9.6	12.2	13.7	11.1	10.2	10.0	10.2	10.5	12.3	11.3	14.0	Incr.	12.7	11.0	12.5	-
2017-2016	7.5	12.6	9.1	13.0	10.9	14.2	11.0	12.3	11.6	12.4	9.8	9.0	8.6	10.6	7.9	10.8	9.5	9.9	9.9	10.6	12.5	10.4	13.7	9.4	10.1	11.3	-



**Fig. 6** Frequency of positive (increased area) and negative (decreased area) of the vegetation change in the filtering zone of the region

Yemen, for example, in addition to January, these are apparent in August and September. Figure 4a shows the average monthly change of vegetation cover, which reveals that the period of March to June, matching the growing season in most parts of the region, has the largest value in comparison with other months. A less sharp increase in average monthly

vegetation land cover from February, a peak during May, and a continual decrease that becomes a minimum by the end of January are also apparent. Figure 4b shows the percentage of time change of vegetation cover in the region. Vegetation cover by the NDVI threshold was generally found in 15 to 20 percent of the total area, such that the lowest percentage of vegetation cover was in 2008 and the highest was in 2010. This result corresponds reasonably with the result of another study done in this region (Khosravi et al. 2017). The density of vegetation cover in the area of each country is shown in Fig. 4c. The highest vegetation land cover density is in Turkey, followed by Iran and the eastern Mediterranean countries (EMC) including Lebanon and Palestine. Figure 4d displays the average monthly NDVI and vegetation cover of the region. It should be noted that the spatial distribution of vegetation cover and the NDVI match, such that the maximum vegetation cover occurs in months when the NDVI > 0.2 is high.

To identify the long-term sustained NDVI, the frequency of pixels with a value greater than 0.2 was identified. A useful way



**Fig. 7** Monthly vegetation change, increasing (green), and decreasing (yellow) in the Middle East over 2001–2017

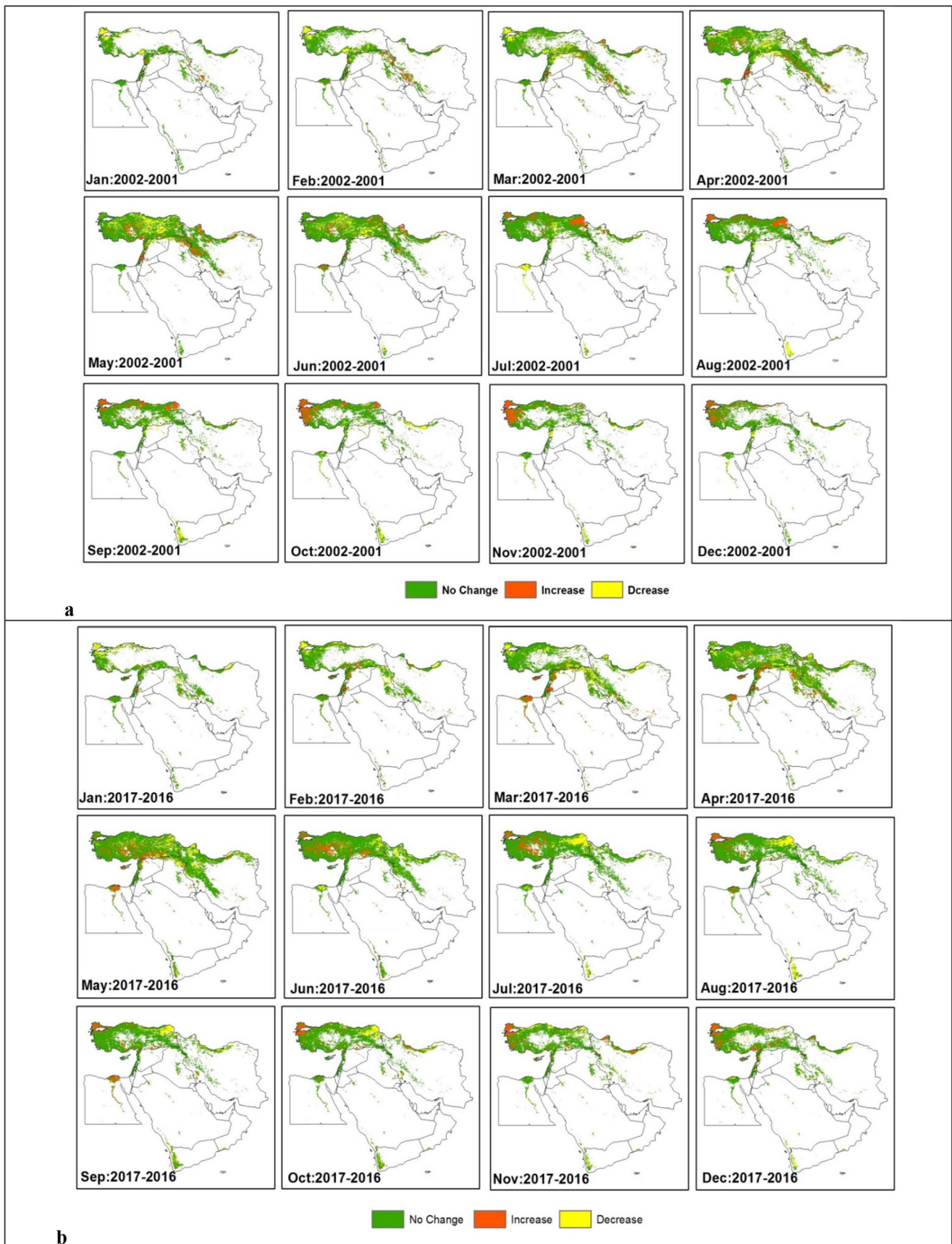


Fig. 8 Representative monthly NDVI differencing, **a** (2002–2001) and **b** (2017–2016)

of defining frequency of pixels is recognition and exploration of the long-term SVC as a scale for reliable vegetation in terms of resistance to drought, which can be reported as pixel counts, percentages, and areas. It is apparent from Fig. 4e that there is a resemblance between the selected pixels and the average monthly vegetation cover description. Figure 4f illustrates the ratio of sustained vegetation area in each year in which the maximum conforms to the year 2008 with lowest vegetation cover over the study period. Therefore, it can be concluded that the SVC shows the minimum drought-tolerant vegetation cover.

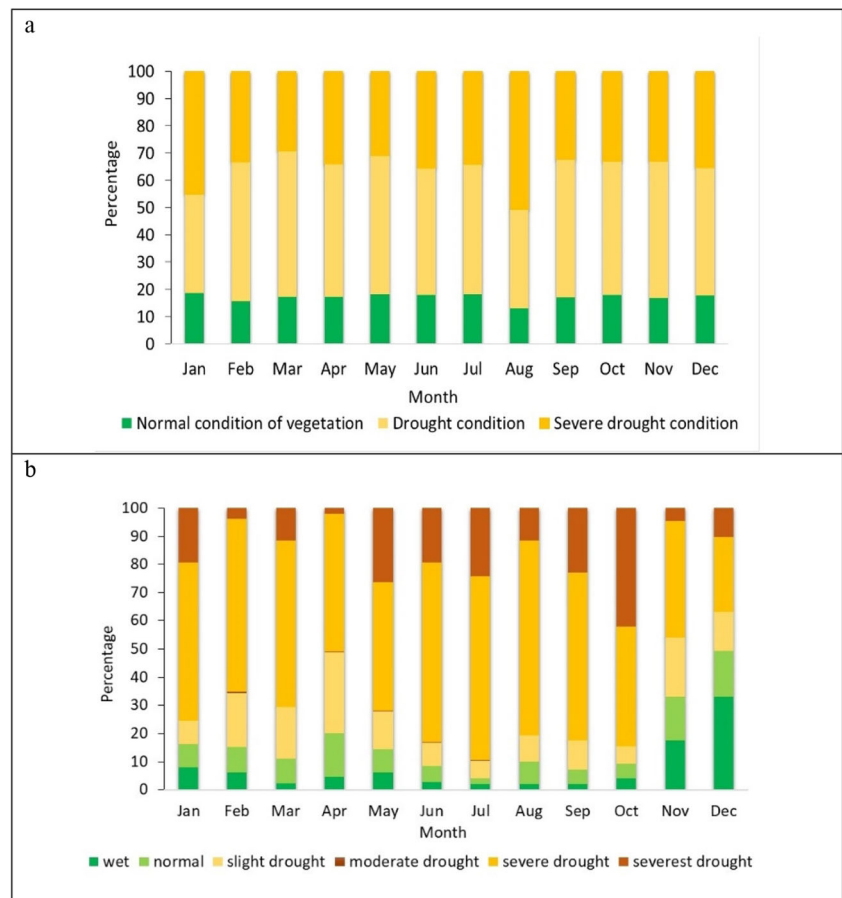
Figure 5a reveals the spatial extent of the monthly mean of sustained NDVI pixel values in the filtering zone of the region from January to May, which can quickly pinpoint the SVC. Figure 5b shows the distribution pattern of the sustained NDVI pixels, which is roughly the same in January, February, and March. The highest frequency distribution of NDVI is in the range of 0.42 to 0.52. Moreover, the number of sustained NDVI pixels increases in February, and this trend is also apparent in March. In April, the highest frequency ranges from 0.3 to 0.4, and as the NDVI increases, the number of pixels decreases. In May and June, the same trend in the distribution of pixels is observed. In May, the highest number of pixels in terms of SVC or sustained pixels always exceeded 0.2 over the course of the study period. In June and August,

the distribution pattern of NDVI values in the sustained pixels is similar and continues until October and November, but their number declined over these months. A significant decrease in the number of pixels is also observed in December (Fig. 5 c, d).

### 3.2 Vegetation change detection

The differencing method generally compares NDVI pixel values, and the NDVI differencing results are then attained by DNDVI by adding a filter threshold to mask water bodies and barren land (Eq. 1). Table 5 shows the percentage of NDVI differencing. The increasing values of vegetation cover range from 7 to 15.7%, and the decreasing values range from 8 to 16.3%. Overall, the vegetation change values show where the trend of average vegetation value is positive, and the probability of a normal year in the year (ni) is much greater than that of the time period (mi). The frequencies of positive and negative changes are shown in Fig. 6. The highest increases are in May 2001 to 2017, and the highest decline occurred in March. The monthly changes (increasing/decreasing) shown in Fig. 7 indicate the highest positive change of percentage of NDVI differencing in most months of the years 2013–2012 and 2015–2014, whereas the highest negative change of percentage of NDVI differencing occurs in most of the months of

**Fig. 9** **a** Comparison of drought and normal VCI during Jan to Dec for the filtering zone of the study area. **b** Comparison of drought and normal NVSWI during Jan to Dec for the filtering zone of the study area



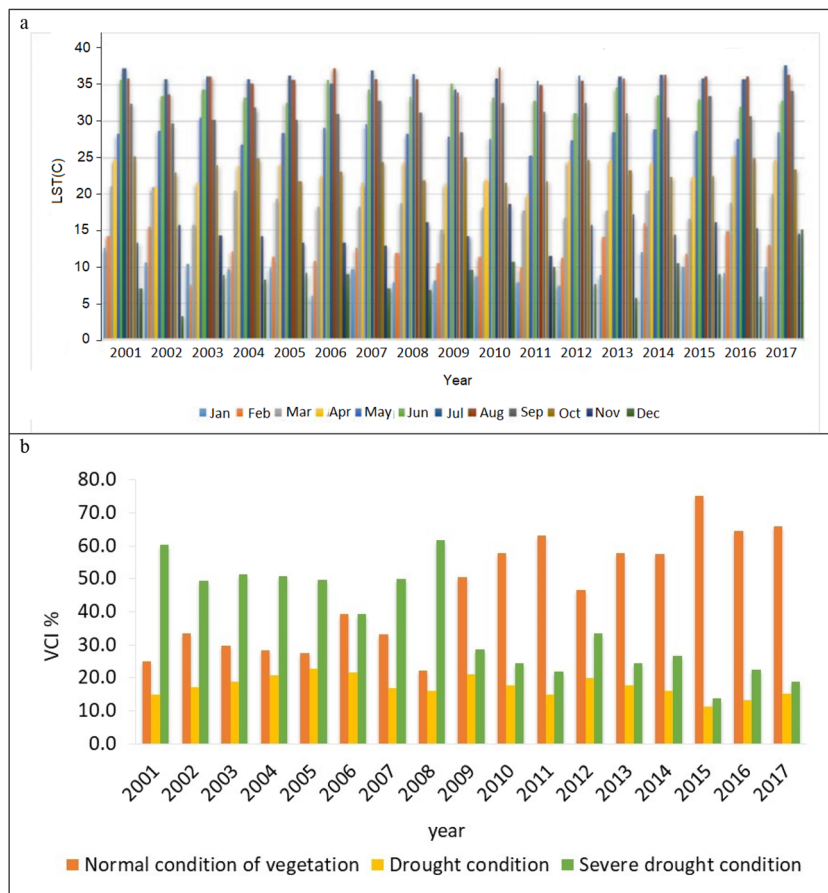
2008–2007. The spatial distribution of these changes for 2002–2001 and 2017–2016 are presented in Fig. 8 as an example.

### 3.3 Drought monitoring

#### 3.3.1 VCI and NVSWI change distribution

The NDVI-derived drought indices from the satellite data, VCI and NVSWI, were used to calculate the drought characteristics of the region. Figure 9a shows the change in distribution of monthly VLC classes over the study area. It was found that water stress and dry conditions prevailed during all months, especially in August, over more than 80% of the area and that less than 20% of the landscape experienced normal vegetation conditions. Presented in Fig. 9b, the NVSWI, as the normalized VSWI, can reveal water stress and a lack of soil moisture. The distribution of the NVSWI shows a pattern similar to that of the VCI for most months; however, in colder periods, such as November, October, January, and April, due to lower LST and evapotranspiration, the percentage of area affected by drought decreases. The LST time series, shown in Fig. 10a, suggests that in warm months, when the surface temperature is increased, the drought condition is intensified.

**Fig. 10** **a** The bar graph of time series of LST (°C) in the filtering zone over 2001–2017. **b** Temporal classification of VCI in the filtering zone of the study area over 2001–2017



In addition, the temporal classification of VCI shown in Fig. 10b reveals a distinct difference between the VCI variation in the year 2008 and that in others, in which around 78% of the filtering zone endured a VCI value below 50, which specifies domination of moderate and severe drought conditions in the region.

#### 3.3.2 Drought change distribution

The SPI and RAI were applied to identify meteorological drought over the study period. The long-term annual precipitation of the region was derived from ERA-Interim precipitation reanalysis data (Borji et al. 2016). Raziei and Sotoudeh (2017) reported that validation of the ERA-Interim indicated a high compliance rate of the reanalysis data with ground-based precipitation and these data have been used instead of observational data. The average SPI and RAI values of the filtering zone are presented in Table 6, which shows the lowest percentage of vegetation cover in the region in the year 2008, in which both meteorological drought indices revealed dominance of drought conditions and the largest decrease in vegetation cover (Nosrati et al. 2009; Khosravi et al. 2017). The highest percentage of SVC or drought-tolerant vegetation has been archived at approximately 73% during the time series of

**Table 6** Percentage change of vegetation cover and drought indexes

Year	Mean NDVI	Mean SPI (Carlson et al. 1994) value	SPI Category	RAI Category	Area ( Km <sup>2</sup> )	Percentage of vegetation cover in ME	Percentage of sustained vegetation/ land cover	Mean of Decrease (%)	Mean of Increase (%)	Year By Year
2001	0.37	-1.79	Severe dryness	Dry	1,172,388	16.599	68			
								10.8	11.7	2002-2001
2002	0.37	0.20	Near Normal	Humid	1194607	16.9	67			
								11.9	10.6	2003-2002
2003	0.37	0.34	Near Normal	Humid	1238207	17.5	64			
								10.8	11.8	2004-2003
2004	0.37	0.69	Near Normal	Humid	1221333	17.3	65			
								11.0	10.5	2005-2004
2005	0.37	0.72	Near Normal	Humid	1208512	17.1	66			
								11.0	11.1	2006-2005
2006	0.38	-1.02	Moderate dryness	Dry	1249691	17.7	64			
								12.0	11.2	2007-2006
2007	0.37	-0.94	Near Normal	Dry	1225502	17.4	65			
								12.6	10.9	2008-2007
2008	0.38	-1.37	Moderate dryness	Very Dry	1090006	15.4	73			
								10.8	12.5	2009-2008
2009	0.39	-0.91	Near Normal	Humid	1217904	17.2	65			
								11.3	11.6	2010-2009
2010	0.39	0.65	Near Normal	Dry	1345374	19.0	59			
								12.2	11.9	2011-2010
2011	0.39	0.07	Near Normal	Humid	1226810	17.4	65			
								12.0	10.9	2012-2011
2012	0.38	0.13	Near Normal	Humid	1197110	16.9	67			
								11.8	12.2	2013-2012
2013	0.39	0.80	Near Normal	Humid	1324267	18.7	60			
								11.7	11.6	2014-2013
2014	0.38	0.44	Near Normal	Humid	1330005	18.8	60			
								11.2	12.5	2015-2014
2015	0.40	0.88	Near Normal	Humid	1354234	19.2	59			
								12.5	11.0	2016-2015
2016	0.39	1.00	Moderate wet	Humid	1325934	18.8	60			
								11.3	10.1	2017-2016
2017	0.38	0.20	Near Normal	Dry	1225811	17.4	65			

the study period. In this research, the meteorological drought indices correspond to the results of SVC and confirm that a large number of sustained NDVI pixels exist even in drought conditions. The effects of drought are clearly evident in the percentage change of vegetation cover in the region.

## 4 Conclusion

In this study, we examined an approach for identifying sustained vegetation cover (SVC) in order to map and monitor

the ME region for a relatively long-term period. The ME is mostly arid and semi-arid land, with sparse vegetation cover in many areas, and drought is a regular phenomenon over the region. Therefore, drought is strongly linked with its consequent effects on vegetation. Hence, considering the SVC may facilitate finding more reliable and realistic results to identify drought conditions. The long-term monthly remotely sensed NDVI and LST of MODIS products were used to extract vegetation and temperature-based drought indices. Because very low NDVI values (i.e., less than 0.2) are identified as non-vegetated areas, this value was used as an optimal

threshold for detecting long-term SVC in order to filter NDVI and classify the confidence levels of the NDVI map. These filtered vegetation maps were used to obtain the SVC, and the performance was assessed by comparing it with the estimated vegetation change, remote sensing-based VCI, and two meteorological drought indices (i.e., SPI and RAI). The results showed the highest severe drought condition and VCL-based drought in 2008 as well as the highest percentage of sustained vegetation cover or highest number of sustained NDVI pixels in this year. Around 75% of the filtering zone endured a VCI value below 50, which indicates the existence of severe drought over the region. A comparison of the estimates of SPI, RAI, vegetation change, and VCI showed that the results were similar to the SVC, which indicates that the drought condition is consistent with the highest increase in sustained vegetation. Despite a reduction of vegetation, an acceptable correlation between SVC and other drought indicators can be attained, which can help to realize resilience of vegetation cover, especially in arid and semi-arid regions, for sustainable natural resources and land management practices. Arid and semi-arid ecosystems have a complex nature, which make it difficult to predict their response to environmental stresses such as drought. The use of remote sensing techniques and vegetation indices is one useful way to understand the ecosystem responses to environmental stresses in a large area better and more rapidly when field data are insufficient. Due to the impact of climate change of increasing drought in the study area, the combined use of the methods of remote sensing and meteorological data can facilitate better understanding and management of land and water resources in the region in both the current situation and the future.

**Acknowledgements** This study was supported by the National Natural Science Foundation of China (grant no. 41625001) and the Strategic Priority Research Program of the Chinese Academy of Sciences (grant no. XDA20060402). It was also partly supported by the High-level Special Funding of the Southern University of Science and Technology (grant nos. G02296302 and G02296402).

**Authors contribution** Elaheh Ghasemi Karakani: methodology, software, and writing of draft manuscript; Arash Malekian: analysis, writing, editing, and reviewing; Soroush Gholami: software analysis; Junguo Liu: reviewing and editing.

## Declarations

**Conflict of interest** The authors declare that they have no conflict of interest.

## References

Abbas S, Nichol JE, Qamer FM, Xu J (2014) Characterization of drought development through remote sensing: a case study in Central Yunnan, China. *Remote Sens* 6:4998–5018. <https://doi.org/10.3390/rs6064998>

- Al-doski J, Mansor SB, Shafri HZM (2013) NDVI differencing and postclassification to detect vegetation changes in Halabja city, Iraq. *IOSR Journal of Applied Geology and Geophysics (IOSR-JAGG)* 1:01–10
- Al-Qinna MI, Hammouri NA, Obeidat MM, Ahmad FY (2011) Drought analysis in Jordan under current and future climates. *Clim Chang* 106:421–440. <https://doi.org/10.1007/s10584-010-9954-y>
- Bannari A, Morin D, Bonn F, Huete A (1995) A review of vegetation indices. *Remote Sens Rev* 13(1):95–120. <https://doi.org/10.1080/02757259509532298>
- Barlow M, Zaitchik B, Paz S, Black E, Evans J, Hoell A (2016) A review of drought in the Middle East and southwest Asia. *J Clim* 29(23): 8547–8574. <https://doi.org/10.1175/JCLI-D-13-00692.1>
- Borji M, Malekian A, Salajegheh A, Ghadimi M (2016) Multi-time-scale analysis of hydrological drought forecasting using support vector regression (SVR) and artificial neural networks (ANN). *Arab J Geosci* 9:725. <https://doi.org/10.1007/s12517-016-2750-x>
- Bucchignani E, Mercogliano P, Panitz H-J, Montesarchio M (2018) Climate change projections for the Middle East–North Africa domain with COSMO-CLM at different spatial resolutions. *Adv Clim Chang Res* 9:66–80. <https://doi.org/10.1016/j.accre.2018.01.004>
- Cai G, Du M, Liu Y (2010) Regional drought monitoring and analyzing using MODIS data—A case study in Yunnan Province, vol 345. Springer, International Conference on Computer and Computing Technologies in Agriculture, pp 243–251
- Cakir HI, Khorram S, Nelson SA (2006) Correspondence analysis for detecting land cover change. *Remote Sens Environ* 102:306–317. <https://doi.org/10.1016/j.rse.2006.02.023>
- Carlson TN, Gillies RR, Perry EM (1994) A method to make use of thermal infrared temperature and NDVI measurements to infer surface soil water content and fractional vegetation cover. *Remote Sens Rev* 9(3–4):161–173. <https://doi.org/10.1080/02757259409532220>
- Coppin P, Jonckheere I, Nackaerts K, Muys B, Lambin E (2004) Digital change detection methods in ecosystem monitoring: a review. *Int J Remote Sens* 25:1565–1596. <https://doi.org/10.1080/0143116031000101675>
- Dee DP, Uppala S, Simmons A, Berrisford P, Poli P, Kobayashi S, Andrae U, Balmaseda M, Balsamo G, Bauer d P (2011) The ERA-Interim reanalysis: Configuration and performance of the data assimilation system. *Q J R Meteorol Soc* 137:553–597. <https://doi.org/10.1002/qj.828>
- Didan K, Munoz AB, Solano R, Huete A (2015) MODIS vegetation index user's guide (MOD13 Series). University of Arizona, Vegetation Index and Phenology Lab
- Dutta D, Kundu A, Patel N, Saha S, Siddiqui A (2015) Assessment of agricultural drought in Rajasthan (India) using remote sensing derived Vegetation Condition Index (VCI) and Standardized Precipitation Index (SPI). *Egypt J Remote Sens Space Sci* 18:53–63. <https://doi.org/10.1016/j.ejrs.2015.03.006>
- Gandhi GM, Parthiban S, Thummalu N, Christy A (2015) NDVI: Vegetation change detection using remote sensing and GIS—a case study of Vellore District. *Proced Computer Sci* 57:1199–1210. <https://doi.org/10.1016/j.procs.2015.07.415>
- Gao M, Qin Z, Zhang HO, Lu L, Zhou X, Yang X (2008) Remote sensing of agro-droughts in Guangdong Province of China using MODIS satellite data. *Sensors* 8:4687–4708. <https://doi.org/10.3390/s8084687>
- Giorgi F, Lionello P (2008) Climate change projections for the Mediterranean region. *Glob Planet Chang* 63:90–104. <https://doi.org/10.1016/j.gloplacha.2007.09.005>
- Gophen M (2008) Lake management perspectives in arid, semi-arid, subtropical and tropical dry climate. *Proceedings of Taal2007: The 12th World Lake Conference*, pp 1338–1348
- Hasanean H (2004) Middle east meteorology. Available online at <https://www.eolss.net/sample-chapters/C01/E6-158-19.pdf>

- Huang K, Zhou T, Zhao X (2014) Extreme drought-induced trend changes in MODIS EVI time series in Yunnan, China. *IOP Conference Series: Earth and Environmental Science* 17(1):012070. <https://doi.org/10.1088/1755-1315/17/1/012070>
- Kafle HK, Bruins HJ (2009) Climatic trends in Israel 1970–2002: Warmer and increasing aridity inland. *Clim Chang* 96:63–77. <https://doi.org/10.1007/s10584-009-9578-2>
- Kaniewski D, Van Campo E, Weiss H (2012) Drought is a recurring challenge in the Middle East. *Proc Natl Acad Sci* 109:3862–3867
- Karnieli A, Agam N, Pinker RT, Anderson M, Imhoff ML, Gutman GG, Panov N, Goldberg A (2010) Use of NDVI and land surface temperature for drought assessment: Merits and limitations. *J Clim* 23: 618–633. <https://doi.org/10.1175/2009JCLI2900.1>
- Khosravi G, Nafarzadegan AR, Nohegar A, Fathizadeh H, Malekian A (2015) A modified distance-weighted approach for filling annual precipitation gaps: application to different climates of Iran. *Theor Appl Climatol* 119(1–2):33–42
- Khosravi H, Haydari E, Shekoozadegan S, Zareie S (2017) Assessment the effect of drought on vegetation in desert area using landsat data. *Egypt J Remote Sens Space Sci* 20:S3–S12. <https://doi.org/10.1016/j.ejrs.2016.11.007>
- Kogan FN (1995) Application of vegetation index and brightness temperature for drought detection. *Adv Space Res* 15:91–100. [https://doi.org/10.1016/0273-1177\(95\)00079-T](https://doi.org/10.1016/0273-1177(95)00079-T)
- Lu D, Mausel P, Brondizio E, Moran E (2004) Change detection techniques. *Int J Remote Sens* 25:2365–2401. <https://doi.org/10.1080/0143116031000139863>
- Magno R, De Filippis T, Di Giuseppe E, Pasqui M, Rocchi L, Gozzini B (2018) Semi-Automatic Operational Service for Drought Monitoring and Forecasting in the Tuscany Region. *Geosciences* 8:49. <https://doi.org/10.3390/geosciences8020049>
- Mancino G, Nolè A, Urbano V, Amato M, Ferrara A (2009) Assessing water quality by remote sensing in small lakes: the case study of Monticchio lakes in southern Italy. *iForest-Biogeosciences and Forestry* 2:154. <https://doi.org/10.3832/ifer0507-002>
- Mancino G, Nolè A, Ripullone F, Ferrara A (2014) Landsat TM imagery and NDVI differencing to detect vegetation change: assessing natural forest expansion in Basilicata, southern Italy. *iForest-Biogeosciences and Forestry* 7:75. <https://doi.org/10.3832/ifer0909-007>
- McKee TB, Doesken NJ, Kleist J (1993) The relationship of drought frequency and duration to time scales. *Proceedings of the 8th Conference on Applied Climatology*, American Meteorological Society Boston, MA, pp 179–183
- Myneni RB, Hall FG, Sellers PJ, Marshak AL (1995) The interpretation of spectral vegetation indexes. *IEEE Trans Geosci Remote Sens* 33: 481–486
- Nosrati K, Eslamian S, Shahbazi A, Malekian A, Mohseni Saravi M (2009) Application of Daily Water Resources Assessment Model for Monitoring Water Resources Indices. *Inter J Ecol Econ Stat* 13(W09):88–99
- Pu R, Gong P, Tian Y, Miao X, Carruthers RI, Anderson GL (2008a) Invasive species change detection using artificial neural networks and CASI hyperspectral imagery. *Environ Monit Assess* 140:15–32. <https://doi.org/10.1007/s10661-007-9843-7>
- Pu R, Gong P, Tian Y, Miao X, Carruthers RI, Anderson GL (2008b) Using classification and NDVI differencing methods for monitoring sparse vegetation coverage: a case study of saltcedar in Nevada, USA. *Int J Remote Sens* 29:3987–4011. <https://doi.org/10.1080/01431160801908095>
- Qader SH, Dash J, Atkinson PM, Galiano V (2016) Classification of vegetation type in Iraq using satellite-based phenological parameters. *IEEE J. Sel. Top. Appl. Earth Obs. Remote Sens* 43: 1–23. <https://doi.org/10.1109/JSTARS.2015.2508639>
- Rahimi J, Malekian A, Khalili A (2018) Climate change impacts in Iran: assessing our current knowledge. *Theor Appl Climatol* 135:545–564
- Raziei T, Sotoudeh F (2017) Investigation of the accuracy of the European Center for Medium Range Weather Forecast (ECMWF) in forecasting observed precipitation in different climates of Iran. *J Earth Space Physics* 43:133–147. <https://doi.org/10.22059/jesphys.2017.57958>
- Richards JA, Jia X (2006) Feature reduction. *Remote sensing digital image analysis: An Introduction*, Springer, pp 267–294
- Sepulcre-Canto G, Horion S, Singleton A, Carrao H, Vogt J (2012) Development of a Combined Drought Indicator to detect agricultural drought in Europe. *Nat Hazards Earth Syst Sci* 12:3519–3531. <https://doi.org/10.5194/nhess-12-3519-2012>
- Shetty S (2006) Water, food security and agricultural policy in the Middle East and North Africa region. *World Bank*, pp 43
- Singh A (1989) Digital change detection techniques using remotely-sensed data. *Int J Remote Sens* 10:989–1003. <https://doi.org/10.1080/01431168908903939>
- Sruthi S, Aslam MM (2015) Agricultural drought analysis using the NDVI and land surface temperature data; a case study of Raichur district. *Aqua Proced* 4:1258–1264. <https://doi.org/10.1016/j.aqpro.2015.02.164>
- Trisasongko BH, Panuju DR, Shiddiq D, La Ode SI, Sholihah RI, KUSDARYANTO S (2015) Constraints of VSWI in the estimation of drought extent using Landsat data: A case of Tuban, Indonesia. *Procedia Environ Sci* 24:25–28. <https://doi.org/10.1016/j.proenv.2015.03.004>
- United Nations (2015) Department of economic and social affairs, population division 2015. *World Population Prospects: The 2015 Revision, Key Findings and Advance Tables*. Working Paper No. ESA/P/WP.241, pp 66
- Van Lanen H, Wanders N, Tallaksen L, Van Loon A (2013) Hydrological drought across the world: impact of climate and physical catchment structure. *Hydrol Earth Syst Sci* 17:1715–1732. <https://doi.org/10.5194/hess-17-1715-2013>
- Van Rooy M (1965) A rainfall anomaly index independent of time and space. *Notos* 14:6
- Wan Z (2008) New refinements and validation of the MODIS Land-Surface Temperature/Emissivity products. *Remote Sens Environ* 112(1):59–74. <https://doi.org/10.1016/j.rse.2006.06.026>
- Wan Z, Wang P, Li X (2004) Using MODIS land surface temperature and normalized difference vegetation index products for monitoring drought in the southern Great Plains, USA. *Int J Remote Sens* 25: 61–72. <https://doi.org/10.1080/0143116031000115328>
- Xie Y, Sha Z, Yu M (2008) Remote sensing imagery in vegetation mapping: a review. *J Plant Ecol* 1:9–23. <https://doi.org/10.1093/jpe/rtn005>
- Zaitchik BF, Evans JP, Geerken RA, Smith RB (2007) Climate and vegetation in the Middle East: interannual variability and drought feedbacks. *J Climate* 20:3924–3941. <https://doi.org/10.1175/JCLI4223.1>
- Zarei A, Asadi E, Ebrahimi A, Jafari M, Malekian A, Mohammadi Nasrabadi H, Chemura A, Maskella G (2020) Prediction of future grassland vegetation cover fluctuation under climate change scenarios. 119:106858. <https://doi.org/10.1016/j.ecolind.2020.106858>

**Publisher's note** Springer Nature remains neutral with regard to jurisdictional claims in published maps and institutional affiliations.